Materials Today Communications 27 (2021) 102451

Contents lists available at ScienceDirect

Materials Today Communications

journal homepage: www.elsevier.com/locate/mtcomm

Atomistic modeling for the extremely low and high temperature-dependent yield strength in a Ni-based single crystal superalloy

Zhiwei Zhang [a,b], Qiang Fu [c], Jun Wang [a,*], Rong Yang [a], Pan Xiao [a], Fujiu Ke [d], Chunsheng Lu [e]

[a] State Key Laboratory of Nonlinear Mechanics (LNM), Institute of Mechanics, Chinese Academy of Sciences, Beijing, 100190, China
[b] School of Engineering Science, University of Chinese Academy of Sciences, Beijing, 100049, China
[c] Aero Engine Academy of China, Beijing, 101304, China
[d] School of Physics, Beihang University, Beijing, 100191, China
[e] School of Civil and Mechanical Engineering, Curtin University, Perth, WA, 6845, Australia

ARTICLE INFO

Keywords:
Ni-based single crystal superalloy
Yield strength
Temperature-dependence
Dislocation activities
Molecular dynamics

ABSTRACT

Understanding the temperature-dependent yield strength of Ni-based single crystal superalloys is of great significance for their microstructural design and engineering applications. In this Communication, from an atomistic perspective, the yield strength of a Ni-based single crystal superalloy varying with temperature, especially at extremely low (−272 °C) and high (1227 °C) temperatures, has been investigated. The atomic-scale mechanisms are elaborated by extracting several types of dislocation activities at various temperatures. The anomalous behavior of yield strength dominated by the atomic-scale dislocation evolution is visualized in Ni-based single crystal superalloys.

1. Introduction

Ni-based single crystal superalloys are widely used to fabricate gas turbine and aircraft engine components in aerospace industries because of their excellent thermomechanical performance and creep, corrosion and oxidation resistance [1,2]. These alloys mainly consist of Ni matrix, Ni_3Al dispersion precipitates and other alloying elements, such as mechanically strengthening elements (B, Re), the long-term stability element (Ru), and oxidation resistance elements (Al, Cr) [3]. Their excellent thermomechanical properties are mainly attributed to the superlattice structure of Ni_3Al precipitates and an interface misfit dislocation (IMD) network, which is created on Ni/Ni_3Al interface due to non-identical lattice parameters of Ni and Ni_3Al. The superlattice structure of Ni_3Al precipitates causes the cross-slip of dislocations, indicating the high-temperature strengthening mechanisms [4,5]. Moreover, the IMD network can absorb and accommodate slip dislocations in Ni matrix, and further impede dislocations in matrix from approaching or shearing into Ni_3Al phase [6,7]. These are the main factors resulting in the emergence of an anomalous yield strength. That is, the yield strength increases with temperatures for Ni-based single crystal superalloys [8,9].

Over the past decades, numerous experiments and theoretical analyses have been carried out to focus on the yield strength anomaly and its intrinsic mechanism in Ni-based single crystal superalloys [10–20]. For example, based on the new directionally solidified Ni-based superalloys M4706 [11], the yield strength anomaly behavior was revealed, which indicates that as temperature is less than 750°C, the anti-phase boundary and stacking fault shearing dominate plastic deformation. Moreover, as temperature is extremely high over 900°C, deformation is achieved mainly with dislocations bypassing Ni_3Al precipitates. Such behaviors were also observed by Tan et al. [12] in ZGD-15 and by Zhang et al. [13] in CMSX-4. However, the yield strength anomaly is also attributed to dislocation cross-slip mechanisms of Ni_3Al precipitates. As temperature is less than that corresponding to the highest yield strength, slip mainly occurs on the octahedral {111} planes. Otherwise, slip on {100} cubic planes becomes dominant [16,17]. Furthermore, several theoretical models for the yield strength anomaly of Ni-base superalloys have been established at elevated temperature, which can possess an amazing predicted ability of experimental results [18,19].

Nevertheless, most of these studies are generally performed on severely deformed or fractured specimens to identify the predominant deformation mechanisms. Due to lack of real-time and in-situ experimental results and a visible dislocation evolution process, it is difficult to have a consensus among these deformation mechanisms. Here it is worth noting that, to the best of our knowledge, there are still no reports on the temperature-dependence of yield strength in Ni-based single crystal

* Corresponding author.
E-mail address: wangjun@lnm.imech.ac.cn (J. Wang).

https://doi.org/10.1016/j.mtcomm.2021.102451
Received 20 April 2021; Received in revised form 12 May 2021; Accepted 12 May 2021
Available online 15 May 2021

superalloys at extremely low temperatures (below 27 °C) and the atomic-scale related mechanism of yield strength anomaly. As is well known, molecular dynamic simulations can be used to elaborate the microstructural evolution in a mechanical process [21,22]. Therefore, in this work, a molecular dynamic method is adopted to comprehensively investigate the influence of temperature on the yield strength of a Ni-based single crystal superalloy, from an extremely low temperature of −272 °C to an elevated temperature of 1227 °C. The densities and activation order of dominant dislocations are extracted to clarify the atomic-scale dislocation evolution mechanism. This work aims to visualize the dislocation activities such as dislocations from Ni matrix interacting with the IMD network and the evolution of an IMD network, which result in the temperature-dependent yield strength of a Ni-based single crystal superalloy.

2. Simulation model and methods

A Ni-based single crystal superalloy consists of pure face-centered cubic Ni matrix and $L1_2$ Ni_3Al precipitate, which cause the mismatch of a Ni/Ni_3Al interfacial lattice. Considering the concept of a coincidence site lattice on misfit interphase interface, there are at least 66 Ni_3Al lattices and 67 Ni lattices to relax stress induced by the difference of lattice parameters with 3.52 Å for Ni and 3.573 Å for Ni_3Al [23,24]. Thus, the volume and shape of a Ni_3Al precipitate structural unit of 66 × 66 × 66 are almost the same as that of a Ni matrix structural unit of 67 × 67 × 67. By substituting the Ni_3Al structural unit for the Ni structural unit in the center of a 75 × 75 × 75 Ni block with the same lattice directions, an initial mosaic cubic model of Ni-based single crystal superalloy can be constructed, as shown in Fig. 1a. The <100> crystallographic orientations are along with three orthogonal coordinates and the model has a volume of 26.4 × 26.4 × 26.4 nm^3 consisting of 1.6 million atoms. In the model, the volume fraction of Ni_3Al is 71 %, which is in agreement with the experimental value of 70 % [2,3]. Due to the lattice misfit of Ni and Ni_3Al, the IMD network can be formed on interphase interface to reduce distorted energy of the system and accommodate the misfit strain [25,26]. The three-dimensional IMD network is formed on the Ni/Ni_3Al {100} interface as illustrated in Fig. 1b.

Atomistic simulations were performed by using the Largescale Atomic/Molecular Massively Parallel Simulator [27]. The embedded-atom potential function for a Ni−Al system developed by Mishin [28] was taken to define atomic interactions of Ni and Ni_3Al. Periodic boundary conditions were implemented in three directions and initial configurations were energetically minimized by relaxing all samples for 100 ps. Tensile simulations were carried out by integrating Newton's equations of motion for all atoms with a time step of 1 fs, and to investigate the temperature effect, temperatures were selected from −272 to 1227 °C. The strain rate was controlled at 5 × 10^8 s^{-1}. The microstructural evolution was recognized via dislocation analysis visualized with software OVITO [29].

3. Results

Fig. 2 shows the tensile stress-strain curves of a Ni-based single crystal superalloy with various temperatures. It is seen that stress linearly increases with strain till reaching the yield strength. To avoid the sample specificity, yield strengths are averaged in five simulations with a diversely initial atomic velocity distribution at a given temperature. The temperature-dependence of yield strength can be divided into three parts, namely low temperature (< 27 °C), intermediate temperature (27–627 °C), and elevated temperature (> 627 °C) zones (see Fig. 3a). In a low temperature zone, the yield strength of a Ni-based single crystal superalloy decreases from 4.9 GPa to its local minimum of 4.2 GPa as temperature increases from −272 to −123 °C, indicating a thermal activation softening process. Then, with temperature rising to 27 °C, it goes up to 4.6 GPa, i.e., the value of yield strength within an intermediate temperature zone, where the yield strength remains almost unchanged with temperature. However, in an elevated temperature zone, as temperature ascends from 627 to 927 °C, yield strength rises and

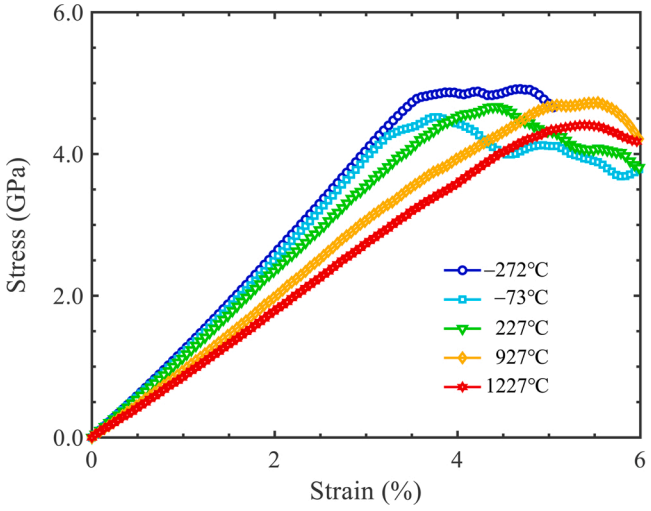

Fig. 2. The stress-strain curves of a Ni-based single crystal superalloy under tension with various temperatures.

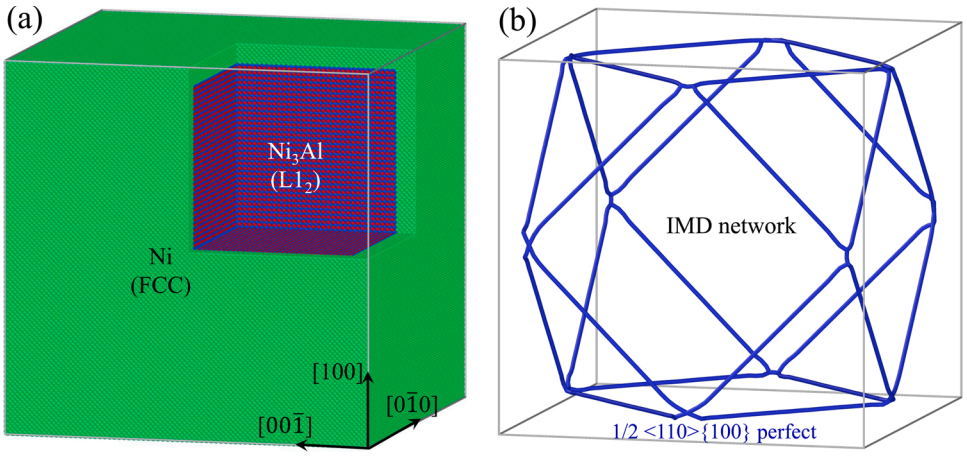

Fig. 1. (a) The initial mosaic cubic model and (b) the IMD network in a Ni-based single crystal superalloy, where atoms were removed for clarity and blue lines indicate the 1/2 <110> perfect dislocations.

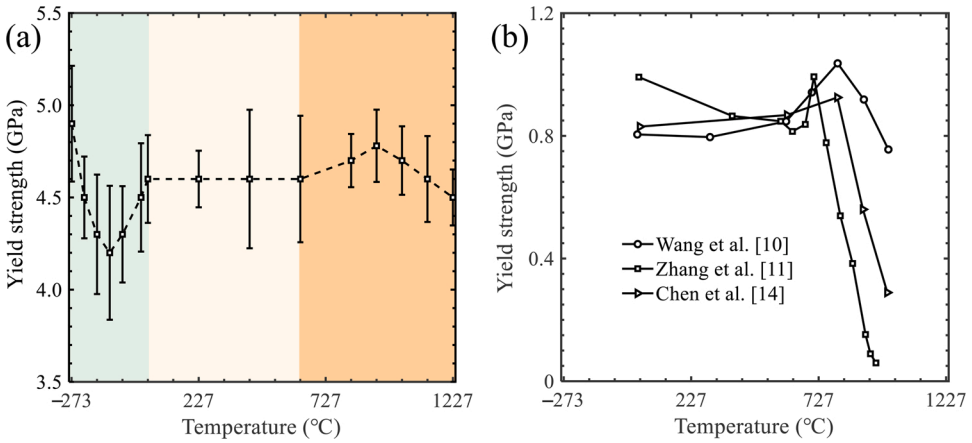

Fig. 3. (a) The yield strength of a Ni-based single crystal superalloy varying with temperature obtained by molecular dynamics simulations and (b) the experimental results of yield strength for Ni-based single crystal superalloys.

reaches its local peak value of 4.8 GPa, showing an anomalous yield strength behavior. After that, as temperature increases to 1227 °C, the yield strength falls to 4.5 GPa. Similar experimental results in intermediate and elevated temperature zones are shown in Fig. 3b.

Real-time detection on densities and activities of dislocations indicates that yield strength is closely related to them as illustrated in Fig. 4. The huge stress overshoots at the yielding point are corresponding to the remarkable dislocation nucleation and growth, which change the density of dominant dislocation lines. Taking cases at −272, −73, 227 and 927 °C as examples, with strain increasing, the densities of 1/6 <110> stair-rod and 1/6 < 112> Shockley dislocation lines first maintain stable. Then, they slightly increase with the yielding point being approached. Finally, they rise sharply at the yielding point. The largest growth rates of 1/6 <112> Shockley dislocation appear at strains of 3.4, 3.8, 4.4 and 5.4 %, which echo precisely the yielding points at four temperatures. However, the density of 1/2 <110> perfect dislocation undergoes exactly an opposite trend due to damage of the original IMD network structure and decomposition of 1/2 <110> perfect dislocations. Specifically, at −272 °C, the IMD network structure consists of purely 1/2 <110> perfect dislocations with a density maintaining at 2.1 × 10^{-4} $Å^{-2}$ in the early elastic stage. It gradually reduces around the yielding point and then tends to stable, indicating decomposition of 1/2 <110> with further increase of strain (see Fig. 4a). At temperatures of −73, 227 and 927 °C, due to temperature-induced relaxation, initial IMD network structures are composed of not only 1/2 <110> perfect but also 1/6 <112> Shockley, 1/6 <110>

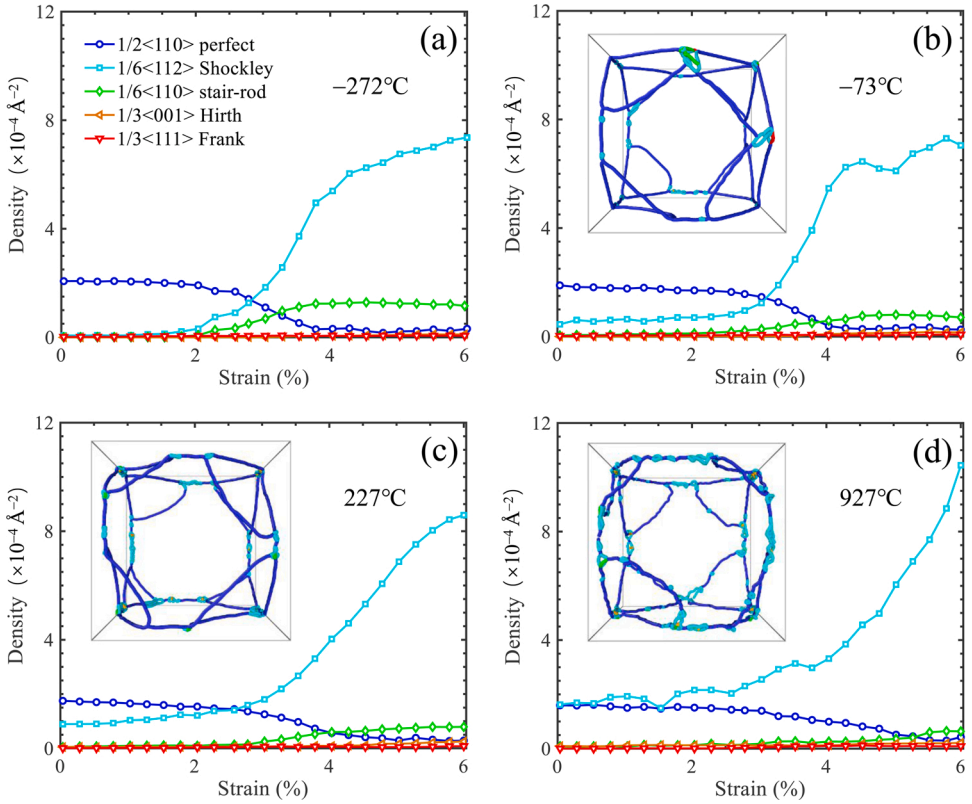

Fig. 4. Evolution of densities of different types of dislocations during tension at various temperatures of (a) −272, (b) −73, (c) 227 and (d) 927 °C. Insets in (b–d) are initial configurations of IMD networks at −73, 227 and (d) 927 °C, respectively, where atoms were removed for clarity and blue, cyan, green, orange, and red lines indicating 1/2 <110> perfect, 1/6 <112> Shockley, 1/6 <110> stair-rod, 1/3 <001> Hirth and 1/3 <111> Frank dislocations.

stair-rod, 1/3 <001> Hirth and 1/3 <111> Frank dislocations (see insets in Fig. 4b–d). The latter three belong to immovable dislocations.

Further analysis reveals that the densities of immovable 1/6 < 110> stair-rod, 1/3 < 001> Hirth, and 1/3 < 111> Frank dislocation lines at yield points depend heavily on temperature, as shown in Fig. 5a. At −272 °C, the density of 1/6 < 110> stair-rods produced by decomposition of 1/2 < 110> perfect on the {111} plane of IMD network is the largest. At the yielding point (strain of 3.4 %), some 1/2 < 110> perfect dislocations on the {111} plane of IMD network begin to decompose. Each dislocation can decompose into one 1/6 < 110> stair-rod and two 1/6 < 112> Shockley dislocations. The reaction can be written as 1/2 [110] → 1/6[110] + 1/6[112] +1/6[11 $\bar{2}$]. Meanwhile, at the intersection of 1/2 < 110> perfect, other 1/6 < 112> Shockley dislocations nucleate on the {111} side plane and expand in the Ni phase (see Fig. 5b). With temperature increasing to 227 °C, the density of 1/3 < 001> Hirth dislocations grows rapidly in comparison with that at other temperatures, declaring its contribution to yield strength in an intermediate temperature zone. The microstructure of IMD network is also partially distorted with part of 1/2 < 110> perfect dislocations decomposing and disappearing gradually. At the same time, the 1/6 < 112> Shockley dislocations from decomposition of 1/2 < 110> perfect on the ($\bar{1}$ 00) plane of IMD network gradually shear into the Ni_3Al precipitate phase and begin to expand to inside (see Fig. 5c). As temperature further reaches 927 °C, 1/3 < 111> Frank dislocations are dominant since their density reaches the maximum in contrast to that at other temperatures. Due to high-temperature thermal activation, the IMD network becomes unstable. More 1/2 < 110> perfect dislocations decompose into 1/6 < 112> Shockley dislocation segments. The interaction of these dislocation segments cause a large number of 1/3 < 111> Frank and 1/3 < 001> Hirth dislocations to exist on the trajectory of the original perfect dislocation of IMD network. Thus, the IMD network is damaged and deformed, with the 1/6 < 112> Shockley dislocation segments on the ($\bar{1}$ 00) plane of the IMD expanding into Ni matrix phase and part of Shockley fragments on the (100) plane of the top surface shearing into Ni_3Al precipitate phase (see Fig. 5d).

4. Discussion

Molecular dynamic simulations show that, in an intermediate temperature zone, the yield strength of a Ni-based single crystal superalloy remains unchanged. In an elevated temperatures zone, however, yield strength first increases to its peak value at 927 °C and then decreases with temperature. This kind of anomalous behavior for Ni-based single crystal superalloys in intermediate and elevated temperature zones are well consistent with experimental results (see Fig. 3b) [10–16]. The discrepancy on yield strengths between our results and experimental tests mainly results from the two facts: One is the strain rate in simulations (5×10^8 s^{-1}) that is much larger than that in experiments (10^{-3}–10^{-2} s^{-1}). It is shown that variation of strain rates with ten orders generates a discrepancy of yield strength by three times [30]. The other is the Ni-based single crystal superalloy model that only contains Ni matrix and Ni_3Al precipitate, while experimental samples contain other alloying elements to tailor yield strength [3]. In a low temperature zone, the yield strength approaches its minimum value at the critical value of temperature, −123 °C. Below the temperature, yield strength decreases with temperature since decomposition of 1/2 <110> perfect dislocations in the IMD network is the main deformation mechanism during a thermal activation process. However, the opposite trend emerges beyond the critical temperature because 1/6 <110> stair-rod and 1/3 <001> Hirth dislocations start to nucleate at the intersection of perfect dislocations and dominate further microstructural evolution of a sample. They are immovable dislocations and form the Hirth and Lomer-Cottrell locks, which contribute to the stability of yield strength with temperature further rising to an intermediate zone [31,32].

Densities of various types of dislocations and dislocation activation order varying with temperature demonstrate that, at an extremely low temperature of −272 °C, the 1/6 <110> stair-rod dislocations generated by decomposition of perfect dislocations are dominant. The activated dislocation slip system is <110> {111} and the maximum yield strength

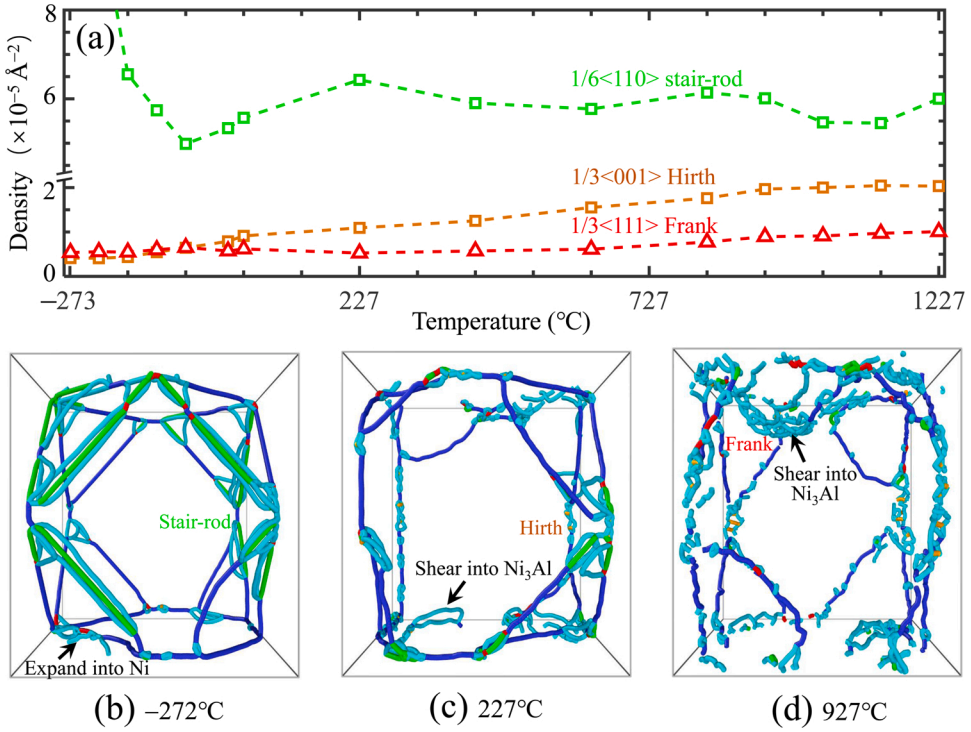

Fig. 5. (a) Densities of various dislocations at yielding points vary with temperature. Atomic configurations of deformed three-dimensional IMD networks at various temperatures of (b) −272, (c) 227 and (d) 927 °C, with atoms being removed for clarity and blue, cyan, green, orange, and red lines indicating 1/2 <110> perfect, 1/6 <112> Shockley, 1/6 <110> stair-rod, 1/3 <001> Hirth and 1/3 <111> Frank dislocations.

is achieved at −272 °C. However, as temperature increases to −123 °C, thermal softening makes such decomposition and slip easier, resulting in reduction of yield strength. These results are consistent with the thermal activation process in materials [33]. Beyond −123 °C, 1/6 <110> stair-rod and 1/3 <001> Hirth dislocations start to take the initiative to nucleate at the corners of IMD network and form dislocations locks to produce pinning effects. This results in yield strength increasing with temperature. In an intermediate temperature zone, dislocation locks formed by 1/3 <001> Hirth and 1/6 <110> stair-rod dislocations have completely controlled the microstructural evolution, generating a stable yield strength. However, in an elevated temperature region, locks formed by 1/3 <111> Frank and 1/3 <001> Hirth dislocations are the main strengthening mechanism, accompanying by lots of 1/6 <112> Shockley dislocation segments on the {100} plane of IMD expanding into Ni phase and shearing into Ni_3Al phase. These phenomena are consistent with the results of Kear–Wilsdorf lock in experimental observations [8,10,13,34], which result in pinning dislocations and improve yield strength.

5. Conclusions

In summary, the temperature-dependence of yield strength in Ni-based single crystal superalloys has been clarified from an atomistic-scale modeling. Analysis on densities and activation order of diverse types of dislocations provides an obvious image of the temperature-dependent yield strength anomalous behavior. It is shown that, as temperature raises from −272 to −123 °C, yield strength first decreases due to thermal softening effect on decomposition of 1/2 <110> to 1/6 <110> and activation of <110> {111} slip system. Then, 1/3 <001> Hirth and 1/6 <110> stair-rod dislocations gradually form locks to promote yield strength until temperature reaches 27 °C. After that, locks formed by 1/3 <001> Hirth and 1/6 <110> stair-rod dislocations play the roles in stabilizing the yield strength as temperature goes up to 627 °C. Finally, nucleation and pinning effects of 1/3 <111> Frank and 1/3 <001> Hirth dislocations push the yield strength to its local peak at 927 °C before thermal softening effect recovers.

Data availability

The data that support the findings within this paper are available from the corresponding author upon reasonable request.

CRediT authorship contribution statement

Zhiwei Zhang: Conceptualization, Investigation, Methodology, Data curation, Writing - original draft. **Qiang Fu:** Formal analysis. **Jun Wang:** Conceptualization, Supervision, Writing - review & editing, Funding acquisition. **Rong Yang:** Funding acquisition, Writing - review & editing. **Pan Xiao:** Methodology, Funding acquisition. **Fujiu Ke:** Methodology. **Chunsheng Lu:** Conceptualization, Writing - review & editing.

Declaration of Competing Interest

The authors declare that they have no known competing financial interests or personal relationships that could have appeared to influence the work reported in this paper.

Acknowledgements

This work has been supported by the National Natural Science Foundation of China (Grant Nos. 11772332 and 11790292), the Strategic Priority Research Program of the Chinese Academy of Sciences (Project No. XDB22040501), and the Opening Fund of State Key Laboratory of Nonlinear Mechanics. The simulations were performed on resources provided by the ScGrid of Supercomputing Center, Computer Network Information Center of the Chinese Academy of Sciences, the LNMGrid of the State Key Laboratory of Nonlinear Mechanics, and the Pawsey Supercomputing Center with funding from the Australian Government and the Government of Western Australia.

References

[1] W.S. Xia, X.B. Zhao, L. Yue, Z. Zhang, Microstructural evolution and creep mechanisms in Ni-based single crystal superalloys: A review, J. Alloys. Compd. 819 (2020), 152954.
[2] A. Pineau, S.D. Antolovich, High temperature fatigue of nickel-base superalloys–a review with special emphasis on deformation modes and oxidation, Eng. Failure Anal. 16 (2009) 2668–2697.
[3] H.B. Long, S.C. Mao, Y.N. Liu, Z. Zhang, X.D. Han, Microstructural and compositional design of Ni-based single crystalline superalloys–a review, J. Alloys. Compd. 743 (2018) 203–220.
[4] R. Maaß, L. Meza, B. Gan, S. Tin, J.R. Greer, Ultrahigh strength of dislocation–free Ni_3Al nanocubes, Small 8 (2012) 1869–1875.
[5] H.X. Xie, B. Liu, Y. Tao, Molecular dynamics simulation of an edge dislocation slipping on a cubic plane of Ni_3Al, Model. Simul. Mater. Sci. Eng. 19 (2011) 065005.
[6] T. Zhu, C.Y. Wang, Misfit dislocation networks in the γ/γ' phase interface of a Ni-based single-crystal superalloy: molecular dynamics simulations, Phys. Rev. B 72 (2005) 014111.
[7] K. Arora, K. Kishida, K. Tanaka, H. Inui, Effects of lattice misfit on plastic deformation behavior of single-crystalline micropillars of Ni-based superalloys, Acta Mater. 138 (2017) 119–130.
[8] Y.M. Wang-Koh, Understanding the yield behaviour of $L1_2$-ordered alloys, Mater. Sci. Technol. 33 (2017) 934–943.
[9] Y. Ru, H.G. Zhao, H. Zhang, X.Y. Pan, W.Y. Zhao, Y.L. Pei, S.S. Li, S.K. Gong, Design for anomalous yield in γ'-strengthening superalloys, Mater. Des. 183 (2019), 108082.
[10] J.J. Wang, W.G. Guo, Y. Su, P. Zhou, K.B. Yuan, Anomalous behaviors of a single-crystal Nickel-base superalloy over a wide range of temperatures and strain rates, Mech. Mater. 94 (2016) 79–90.
[11] P. Zhang, Y. Yuan, S.C. Shen, B. Li, R.H. Zhu, G.X. Yang, X.L. Song, Tensile deformation mechanisms at various temperatures in a new directionally solidified Ni-base superalloy, J. Alloys. Compd. 694 (2017) 502–509.
[12] Z.H. Tan, X.G. Wang, Y.L. Du, T.F. Duan, Y.H. Yang, J.L. Liu, L. Yang, J.G. Li, Y. Z. Zhou, X.F. Sun, Temperature dependence on tensile deformation mechanisms in a novel Nickel-based single crystal superalloy, Mater. Sci. Eng. A 776 (2020) 138997.
[13] H. Zhang, Q.Y. Wang, X.F. Gong, T.J. Wang, W. Zhang, K. Chen, C. Wang, Y.J. Liu, Q.Y. Wang, Dependence on temperature of compression behavior and deformation mechanisms of nickel-based single crystal CMSX-4, J. Alloys. Compd. 866 (2021), 158878.
[14] L. Chen, W.D. Wen, H.T. Cui, H.J. Zhang, Y. Xu, Yield anisotropy and tension/compression asymmetry of a Ni_3Al based intermetallic alloy, Chin. J. Aeronaut. 26 (2013) 801–806.
[15] X.W. Li, J.S. Liang, T. Shi, D.N. Yang, X.C. Chen, C.W. Zhang, Z.H. Liu, D.Z. Liu, Q. X. Zhang, Tribological behaviors of vacuum hot-pressed ceramic composites with enhanced cyclic oxidation and corrosion resistance, Ceram. Int. 46 (2020) 12911–12920.
[16] A. Sengupta, S.K. Putatunda, L. Bartosiewicz, J. Hangas, P.J. Nailos, M. Peputapeck, F.E. Alberts, Tensile behavior of a new single-crystal nickel-based superalloy (CMSX-4) at room and elevated temperatures, J. Mater. Eng. Perform. 3 (1994) 73–81.
[17] P.H. Thornton, R.G. Davies, T.L. Johnston, The temperature dependence of the flow stress of the γ' phase based upon Ni_3Al, Metall. Trans. 1 (1970) 207–218.
[18] P.J. Geng, W.G. Li, X.H. Zhang, Y. Deng, H.B. Kou, J.Z. Ma, J.X. Shao, L.M. Chen, X. Z. Wu, A theoretical model for yield strength anomaly of Ni-base superalloys at elevated temperature, J. Alloys. Compd. 706 (2017) 340–343.
[19] W.G. Li, J.Z. Ma, H.B. Kou, J.X. Shao, X.Y. Zhang, Y. Deng, Y. Tao, D.N. Fang, Modeling the effect of temperature on the yield strength of precipitation strengthening Ni-base superalloys, Int. J. Plast. 116 (2019) 143–158.
[20] X.W. Li, T. Shi, B. Li, X.C. Chen, C.W. Zhang, Z.G. Guo, Q.X. Zhang, Subtractive manufacturing of stable hierarchical micro-nano structures on AA5052 sheet with enhanced water repellence and durable corrosion resistance, Mater. Des. 183 (2019), 108152.
[21] F. Shuang, K.E. Aifantis, Relating the strength of graphene/metal composites to the graphene orientation and position, Scr. Mater. 181 (2020) 70–75.
[22] Z.W. Zhang, Q. Fu, J. Wang, R. Yang, P. Xiao, F.J. Ke, C. Lu, Interactions between butterfly-like prismatic dislocation loop pairs and planar defects in Ni_3Al, Phys. Chem. Chem. Phys. 23 (2021) 10377–10383.
[23] Z.W. Zhang, Q. Fu, J. Wang, P. Xiao, F.J. Ke, C. Lu, Hardening Ni_3Al via complex stacking faults and twinning boundary, Comput. Mater. Sci. 188 (2021) 110201.
[24] A.F. Voter, S.P. Chen, Accurate interatomic potentials for Ni, Al and Ni_3Al, MRS Proc. 82 (1986) 175.
[25] S.G. Tian, H.H. Zhou, J.H. Zhang, H.C. Yang, Y.B. Xu, Z.Q. Hu, Formation and role of dislocation networks during high temperature creep of a single crystal nickel-base superalloy, Mater. Sci. Eng. A 279 (2000) 160–165.
[26] W.P. Wu, Y.F. Guo, Y.S. Wang, R. Mueller, D. Gross, Molecular dynamics simulation of the structural evolution of misfit dislocation networks at γ/γ' phase interfaces in Ni-based superalloys, Philos. Mag. 91 (2011) 357–372.

[27] S. Plimpton, Fast parallel algorithms for short-range molecular dynamics, J. Comput. Phys. 117 (1995) 1–19.
[28] Y. Mishin, Atomistic modeling of the γ and γ′ phases of the Ni–Al system, Acta Mater. 52 (2004) 1451–1467.
[29] A. Stukowski, Visualization and analysis of atomistic simulation data with OVITO-the Open Visualization Tool, Model. Simul. Mater. Sci. Eng. 18 (2009) 015012.
[30] T. Zhu, J. Li, A. Samanta, A. Leach, K. Gall, Temperature and strain-rate dependence of surface dislocation nucleation, Phys. Rev. Lett. 100 (2008), 025502.
[31] G. Schoeck, Interaction of Lomer-Cottrell locks with screw dislocations, Philos. Mag. 90 (2010) 629–636.
[32] Z.G. Yan, Y.J. Lin, Lomer-Cottrell locks with multiple stair-rod dislocations in a nanostructured Al alloy processed by severe plastic deformation, Mater. Sci. Eng. A 747 (2019) 177–184.
[33] P. Chen, Z.W. Zhang, C.S. Liu, T. An, H.P. Yu, F. Qin, Temperature and grain size dependences of mechanical properties of nanocrystalline copper by molecular dynamics simulation, Model. Simul. Mater. Sci. Eng. 27 (2019) 065012.
[34] P.B. Hirsch, Kear-Wilsdorf locks, jogs and the formation of antiphase-boundary tubes in Ni_3Al, Philos. Mag. 74 (1996) 1019–1040.